International Journal on Magnetic Particle Imaging
Vol 6, No 2, Suppl 1, Article ID 2009023, 3 Pages

Infinite Science Publishing

*Proceedings Article*

# Estimating orientation using multi-contrast MPI

M. Möddel[1,2,*] · F. Griese[1,2] · T. Kluth[3] · T. Knopp[1,2]

[1]Section for Biomedical Imaging, University Medical Center Hamburg-Eppendorf, Hamburg, Germany
[2]Institute for Biomedical Imaging, Hamburg University of Technology, Hamburg, Germany
[3]Center for Industrial Mathematics, University of Bremen, Bremen, Germany
[*]Corresponding author, email: m.hofmann@uke.de



**Abstract**

Magnetic particle imaging (MPI) is a tracer based tomographic imaging technique that uses static and oscillating magnetic fields to generate an image contrast from the spatial distribution of magnetic nanoparticles. Recent investigations have shown that the MPI is able to generate additional contrasts from different tracer materials or their environments. For example, multi-contrast MPI can be used to determine the viscosity or temperature of the particle environment, or to distinguish tracer particles based on their core size. In this work, we investigate a novel contrast based on the magnetic anisotropy of immobilized particles which allows to estimate the orientation of samples.

## I Introduction

In MPI magnetic nanoparticles are used as tracer material. Static and oscillating magnetic fields cause the ensemble magnetization of the tracer particles to react with a magnetization signal which encodes information about the spatial distribution [1], properties [2] and environment [2] of the tracer particles. Recent investigations have shown that temperature [3] and viscosity [4,5] can be recovered from the magnetization signal.

The magnetic response of the magnetic nanoparticles is governed by a mixture of the internal reorientation of the magnetic moment (Néel rotation) and reorientation of the particle itself (Brownian rotation) [6]. When nanoparticles are immobilized, Néel rotation dominates the particles magnetization dynamics. Recently, it has been shown that the orientation of the magnetic easy axis influences the magnetization dynamics of magnetic nanoparticles [7] and that it plays a key role for proper modeling the system function for multi-dimensional excitation patterns [8]. We use these findings to establish a new MPI contrast that allows to estimate the orientation of the easy axis and thereby the orientation of a sample of immobilized nanoparticles with aligned easy axis.

## II Material and methods

Perimag (micromod Partikeltechnologie GmbH, Rostock, Germany) nanoparticles with an iron concentration of 50 $\mathrm{mmol_{Fe}L\text{-}1}$ was used as MPI tracer. Containers with a cylindrical recess of radius 1.7 mm and height 1.5 mm were 3D printed to prepare four samples with immobilized and magnetic easy axis radially aligned nanoparticles. To this end dental cement and 13.5 $\mu$L of the tracer were added into the cylindrical recess of each container. Immobilization of the nanoparticles and alignment of the magnetization easy axis was done by curing the dental cement in a static homogeneous magnetic field. Additionally, a three-point phantom was 3D printed, where three samples can be placed on the y-axis of our MPI

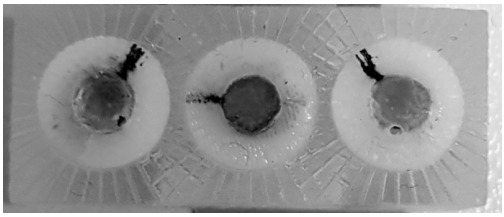

**Figure 1:** The three-point phantom with samples aligned at 120°, 0°, and 60° (left to right) is shown.

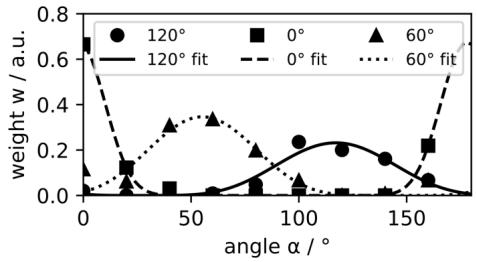


**Figure 2:** Exemplarily, the weights (markers) of the first measurement in which the samples are aligned at 60°, 0°, and 120°, are shown in dependence of the channel labeled by the alignment of the delta sample. Fitting curves (lines) provide an estimate of the alignment of the easy axes of 50°, 178°, and 110°.

system centered at −8 mm, 0 mm, and 8 mm and aligned individually as shown in Fig. 1.

2D MPI measurements were performed with a preclinical system (Philips preclinical MPI package with a Bruker preclinical MPI system) operated with a gradient strength of $-1\,\mathrm{T}\mu_0^{-1}\mathrm{m}^{-1}$ in $x$- and $y$-directions, $2\,\mathrm{T}\mu_0^{-1}\mathrm{m}^{-1}$ in $z$-direction, and a drive-field amplitude of $12\,\mathrm{mT}\mu_0^{-1}$ in $x$- and $y$-directions, where $\mu_0$ is the vacuum permeability. The system uses a field free point Lissajous trajectory with 2.5/102 MHz and 2.5/99 MHz excitation frequencies. The trajectory covers a 24x24 mm$^2$ field of view and has a repetition time of 652.8 $\mu$s. For signal reception we use a custom receive chain with a single gradiometric pickup coil aligned parallel to the $x$-axis of our MPI system.

Nine different system matrices were measured using sample 1 as delta sample on a 30x30 voxel grid covering a field of view of 30x30 mm$^2$. At each position 500 MPI cycles were averaged to increase the signal to noise ratio. For each system matrix the magnetic easy axis of sample 1 was rotated within the $xy$-plane to enclose an angle of 0° to 160° in 20° steps to the $x$-axis, respectively. The three-point phantom centered in the field of view was used to measure the three remaining samples for 10000 excitation cycles aligned at 0°, 60°, and 120° using all possible permutations for sample placement at -8 mm, 0 mm, and 8 mm on the $y$-axis, respectively.

All measurements were block averaged with a block size of 500 and reconstructed using all 9 system matrices

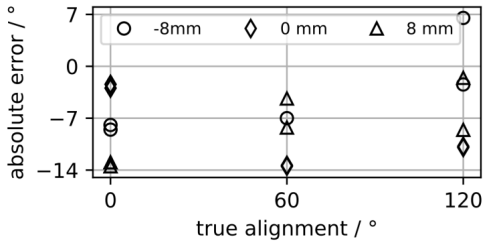


**Figure 3:** The mean absolute estimation error is shown for all measurements. Two values are available for each alignment and position due to the permutation of the sample position in the measurement protocol. The mean is taken with respect to the 20 images reconstructed per measurement. A single outlier (-8 mm) at −32° for 60° alignment is not shown.

in a multi-channel reconstruction approach [9]. To this end, we used our open source reconstruction framework [10], a signal-to-noise threshold of 3, a relative Tikhonov regularization parameter of 0.01, and 10000 iterations. This yields a total of 20 9-channel images per measurement, where each channel corresponds to one of the system matrices, which we will refer to by the alignment of the corresponding delta sample.

To estimate the angle of a sample from the multi-channel image, we propose the following: A circular region of interest (ROI) with a radius of 4 voxels is created at the image location of the sample. The signal within the ROI is summed up for each channel individually yielding 9 weights each corresponding to a specific alignment of the delta sample as shown is Fig. 2. These weights are least squares fitted by

$$w(\alpha) = a\left(\left(\cos\frac{\pi(\alpha-\alpha_e)}{180°}\right)^2\right)^b, \tag{1}$$

where $\alpha$ is the delta sample alignment angle and $a$, $\alpha_e$, and $b$ are model parameters. The maximum of the fitting curve at $\alpha_e$ is taken as estimate for the axis alignment.

## III Results and discussion

Easy axis alignments were estimated for all measurements and samples in the phantom and are summarized in Fig. 3. A single strong outlier estimating the 60° alignment to be 28° for the sample located at -8 mm was observed and excluded from further analysis. The alignments 0°, 60°, and 120° were estimated to be -8(5)°, 51(4)°, and 115(7)°, respectively. Within a measurement alignment estimates showed only a marginal spread with standard deviation below 1° stemming from image noise. In stark contrast, we observed a systematic underestimation of the true alignment of on average 7°. As for the position of the sample no spatial dependence on the alignment estimation could be observed.

10.18416/ijmpi.2020.2009023

In this study, the main source of error is the alignment of the samples by a marker on a set of auxiliary lines available at 10° intervals. The impact of this error is twofold, as the sample was aligned during the curing process of the dental cement and preparation of the phantom or delta sample. A systematic misalignment of the easy axis in sample 1 compared to the other three is the most likely explanation for the systematic underestimation observed. Likewise, the inaccuracy of the alignment estimates of up to 7° is dominated by the alignment process. In practice, it is therefore important to improve the experimental setup with respect to alignment accuracy, which may improve accuracy to the 1° limited by image noise.

Beyond what we presented here, it should be possible to generalize the method to estimate 3D alignments rather than in plane alignments. To this end, it could be of interest to investigate the impact additional receive channels and the excitation trajectory have when it comes to encode the easy axis alignment into the MPI signal.

## IV Conclusions

In this work, we provided a proof of principle that the alignment of the easy axis provides a novel imaging contrast for multi-contrast MPI. We have shown that this contrast can be used to estimate the alignment of samples with immobilized nanoparticles with aligned easy axis. Among the other imaging contrasts it is the only one enabling pose estimation which is highly beneficial for dedicated applications such as the navigation of catheters, magnetic swimmers [11], and other medical devices.

## References

[1] B. Gleich and J. Weizenecker, Tomographic imaging using the nonlinear response of magnetic particles, Nature, vol. 435, 2005.

[2] J. Rahmer, A. Halkola, B. Gleich, I. Schmale, and J. Borgert, First experimental evidence of the feasibility of multi-color magnetic particle imaging, Phys. Med. Biol., vol. 60, pp. 1775–1791, 2015.

[3] C. Stehning, B. Gleich, and J. Rahmer, Simultaneous magnetic particle imaging (MPI) and temperature mapping using multi-color MPI, Int. J. Magn. Part. Imaging, vol. 2, 2016.

[4] M. Möddel, C. Meins, J. Dieckhoff, and T. Knopp, Viscosity quantification using multi-contrast magnetic particle imaging, New J. Phys., vol. 20, 083001, 2018.

[5] M. Utkur, Y. Muslu, and E. U. Saritas, Relaxation-based color magnetic particle imaging for viscosity mapping, Appl. Phys. Lett., vol. 115, 152403, 2019.

[6] S. A. Shah, D. B. Reeves, R. M. Ferguson, J. B. Weaver, and K. M. Krishnan, Mixed Brownian alignement and Néel rotations in superparamagnetic iron oxide nanoparticle suspensions driven by an ac field, Phys. Rev. B, vol. 92, 094438, 2015.

[7] T. Yoshida, et al., Effect of alignment of easy axes on dynamic magnetization of immobilized magnetic nanoparticles, J. Magn. Magn. Mater., vol. 427, pp. 162-167, 2017.

[8] T. Kluth, P. Szwargulski, and T. Knopp. Towards accurate modeling of the multidimensional magnetic particle imaging physics, New J. Phys., vol. 21, 103032, 2019.

[9] J. Rahmer, A. Halkola, B. Gleich, and J. Borgert, First experimental evidence of the feasibility of multi-color magnetic particle imaging, Phys. Med. Biol., vol. 60, pp. 1775–91, 2015.

[10] T. Knopp, P. Szwargulski, F. Griese, M. Grosser, M. Boberg, and M. Möddel, MPIReco.jl: Julia package for image reconstruction in MPI, Int. J. Mag. Part. Imag., vol. 4, 2, 2019.

[11] A. C. Bakenecker, et al., Actuation and visualization of a magnetically coated swimmer with magnetic particle imaging, J. Magn. Magn. Mater., vol. 473, pp. 495-500, 2019.

10.18416/ijmpi.2020.2009023